Modeling the effect of control on the wake of a utility-scale turbine via large-eddy simulation

Xiaolei Yang[a], Jennifer Annoni[b], Pete Seiler[b], and Fotis Sotiropoulos[a,*]

[a] St. Anthony Falls Laboratory, Department of Civil Engineering, University of Minnesota, 2 Third Avenue SE, Minneapolis, MN 55414, USA

[b] Aerospace and Engineering Mechanics Department, University of Minnesota, 110 Union St. SE, Minneapolis, MN 55455, USA

[*] Corresponding author: fotis@umn.edu

Abstract. A model of the University of Minnesota EOLOS research turbine (Clipper Liberty C96) is developed, integrating the C96 torque control law with an actuator line large-eddy simulation (LES). Good agreement with the blade-element momentum theory is obtained for the power coefficient curve under uniform inflow. Three different cases, fixed rotor rotational speed ω, fixed tip-speed ratio (TSR) and generator torque control, have been simulated for turbulent inflow. With approximately the same time-averaged ω, the time-averaged power is in good agreement with measurements for all three cases. Although the time-averaged aerodynamic torque is nearly the same for the three cases, the root-mean-square (rms) of the aerodynamic torque fluctuations is significantly larger for the case with fixed ω. No significant differences have been observed for the time-averaged flow fields behind the turbine for these three cases.

1. Introduction

Individual turbines currently operate at their peak efficiency without considering the impact of wake effects on nearby turbines. This mode of operation leads to inefficient, sub-optimal power capture at the wind farm level. There is great potential to increase total power and reduce structural loads by properly coordinating the turbines in a farm. The effective design of such coordinated controllers requires an accurate model of the fluid dynamics within the wind farm.

Several studies can be found in literature for large-eddy simulation (LES) with turbines parametrized as actuator lines/disks and turbine controller. In [1], the FAST [2] was coupled with an LES code and an actuator disk model. In SOWFA (Simulator for Offshore/Onshore Wind Farm Applications) [3, 4, 5, 6] developed by the National Renewable Energy Laboratory (NREL), OpenFOAM [7] was coupled with FAST and an actuator line model. Applications of SOWFA can be found in [4] for investigation of the effects of atmospheric stability and surface roughness on turbine wake aerodynamics. In addition, [8] investigates the effects of turbine-array layout on wind farm performance. Others [9] coupled SOWFA with WRF (Weather Research and Forecasting Model), in which the WRF provides the LES with initial flow fields. Lastly [10, 11] used SOWFA for validation of dynamic wake meandering model. Wake mitigation control strategies, including yaw misalignment and tilt angle of an upstream turbine, repositioning of the downstream turbine and independent pitch control (IPC) for mitigating the effects of a partial wake for a two-turbine case was also investigated in [12] using SOWFA.

As a first step to develop advanced turbine controllers on wind farm level, we implement the generator torque control in the actuator line model of VWiS (Virtual Wind Simulator), a high-fidelity LES framework developed in Saint Anthony Fall Laboratory, University Minnesota, MN, USA, and use the University of Minnesota's 2.5MW EOLOS research wind turbine (C96) as the turbine model in the simulator. The rotating speed of a turbine rotor can be fixed, from a fixed tip-speed ratio and oncoming wind velocity, or governed by a control law. The objective of this paper is to examine how these different operating conditions affect the turbine performance and also the wake behaviour of the EOLOS turbine.

2. Numerical methods

2.1. Flow solver

The LES equations governing the incompressible turbulent flows are the 3D, unsteady, filtered continuity and Navier-Stokes equations. The curvilinear immersed boundary (CURVIB) method [13] is used to solve these equations in order to facilitate future extension of the method to simulate topography effects. In this method the governing equations are first written in Cartesian coordinates x_i and then transformed fully (both the velocity vector and spatial coordinates are expressed in curvilinear coordinates) in non-orthogonal, generalized, curvilinear coordinates ξ^i. The transformed equations read in compact tensor notation (repeated indices imply summation) as follows $(i, j = 1, 2, 3)$,

$$J\frac{\partial U^j}{\partial \xi^j} = 0, \tag{1}$$

$$\begin{aligned}\frac{1}{J}\frac{\partial U^i}{\partial t} =& \frac{\xi_l^i}{J}\left(-\frac{\partial}{\partial \xi^j}(U^j u_l) + \frac{\mu}{\rho}\frac{\partial}{\partial \xi^j}\left(\frac{g^{jk}}{J}\frac{\partial u_l}{\partial \xi^k}\right)\right.\\ &\left.-\frac{1}{\rho}\frac{\partial}{\partial \xi^j}(\frac{\xi_l^j p}{J}) - \frac{1}{\rho}\frac{\partial \tau_{lj}}{\partial \xi^j} + f_l\right),\end{aligned} \tag{2}$$

where $\xi_l^i = \partial\xi^i/\partial x_l$ are the transformation metrics, J is the Jacobian of the geometric transformation, u_i is the i^{th} component of the velocity vector in Cartesian coordinates, $U^i{=}(\xi_m^i/J)u_m$ is the contravariant volume flux, $g^{jk} = \xi_l^j\xi_l^k$ are the components of the contravariant metric tensor, ρ is the density, μ is the dynamic viscosity, p is the pressure, $f_l(l = 1, 2, 3)$ are the body forces introduced by the wind turbines and τ_{ij} represents the anisotropic part of the subgrid scale stress tensor, which is modelled by the dynamic Smagorinsky subgrid scale model [14]. For details of the CURVIB method and numerical schemes, please refer to the papers [13, 15].

2.2. Actuator line model with generator torque control

The actuator line model [16] is employed for turbine parametrization. The actuator line model accounts for the blades as separate rotating lines. The forces distributed on each line (blade) are calculated based on a blade element approach, in which the blade is divided into elements in the radial direction, and tabulated as 2D airfoil data. The smoothed 4-point discrete delta function proposed in [17] is employed for force distribution from the actuator line grid nodes to the background grid nodes. For more details about the formulation and numerical implementation of the discrete delta function in turbine parametrization models the reader is referred to [18, 19].

Utility-scale turbines have several inputs that can be controlled to increase the captured power and reduce structural loads. These inputs include generator torque, τ_g, and blade pitch, β, at varying wind speeds, u, which can control the rotor speed of the turbine, ω (Figure 1). In general, the generator torque is varied at low wind speeds (commonly referred to as Region 2)

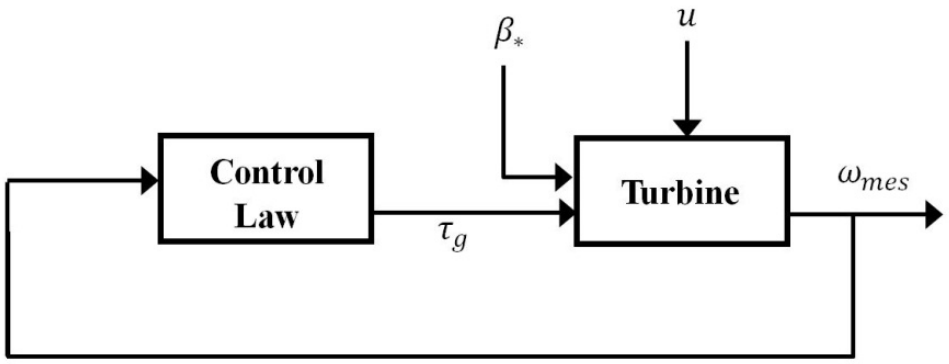

Figure 1: Block Diagram of a Standard Turbine Controller in Low Wind Speeds (Region 2).

to maximize power captured. At high wind high wind speed (commonly called Region 3), the blade pitch angle is used to mitigate mechanical and electrical loads.

A standard generator torque controller, which is used at low wind speeds, is considered in this paper. The power captured by a single turbine can be expressed by:

$$P = \frac{1}{2}\rho A U^3 C_P(\beta, \lambda) \tag{3}$$

where ρ $[kg/m^3]$ is the air density, A $[m^2]$ is the area swept by the rotor, U [m/s] is the wind speed perpendicular to the rotor plane, and C_P [unitless] is the power coefficient. The power coefficient is the fraction of available power in the wind captured by the wind turbine. C_P is a function of blade pitch angle, β [rad] and nondimensional tip-speed-ratio (TSR). TSR is defined as $\lambda = \omega R/U$ where ω [rad/s] is the rotor speed and R [m] is the rotor radius. The peak C_{P*} value is achieved at some fixed blade pitch angle, β_* and an optimal TSR, λ_*. Under realistic conditions, the blade pitch angle can be held constant at β_*, while TSR varies with varying wind speed. The optimal TSR, λ_*, can be achieved by changing the rotor speed proportionally to the wind variations. The objective of a generator torque controller is to maximize power. This is done by maintaining an optimal blade pitch angle (β_*) and TSR (λ_*). The blade pitch angle is held fixed at β_*, and the generator torque is controlled to achieve λ_* in varying wind conditions. The dynamics of the turbine are modelled as a single degree-of-freedom rotational system:

$$\frac{d\omega}{dt} = \frac{1}{J}(\tau_{aero} - \tau_g) \tag{4}$$

where J is the rotational inertial of the rotor, τ_{aero} [Nm] is the aerodynamic torque given by the actuator line model, and τ_g [Nm] is the generator torque, which can be computed using the standard control law:

$$\tau_g = K_g \omega^2 \tag{5}$$

where $K_g = \frac{1}{2}\rho A R^3 \frac{C_{P*}}{\lambda_*^3 N}$ and N is the gearbox ratio. If K_g is chosen properly, the power from the turbine will converge to C_{P*} in steady winds. In turbulent winds, the turbine will cycle around the peak λ_*. Additional details and references on turbine control can be found in [20, 21, 22].

3. Numerical results

We apply our method to simulate a Clipper Liberty 2.5MW wind turbine, the centrepiece of the EOLOS wind energy research field station, which is installed at UMore Park in Rosemount, MN (about 20 miles southeast of the Twin Cities campus). The rotor diameter of the turbine

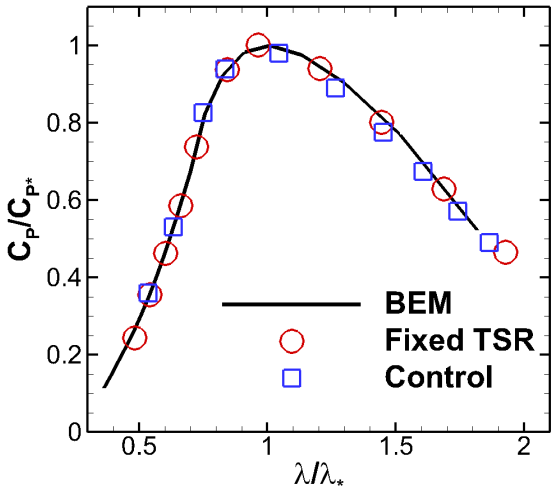

Figure 2: Power coefficients calculated from uniform flow. Solid black line: blade element theory, red circles: different fixed TSR, blue squares: generator torque control with different K_g.

is 96 meters at a hub height of 80 meters. A 130-meter-tall meteorological tower is located at 160 meters south of the turbine. Instruments are installed at 10 different heights on the tower spanning the entire swept area of the turbine blades, in which four with sonic anemometers measuring wind speed and turbulence at a very rapid sampling rate, and six with temperature, barometric pressure and humidity sensors as well as cup and vane anemometers. The turbine's Supervisory Control and Data Acquisition (SCADA) system is employed to record the operational and performance data from the turbine. The measurements for comparison were taken from 11:20 am to 12:20 pm on May 19, 2012. In this case, the atmospheric stability is neutral. The wind is from the south with a time-averaged streamwise velocity at hub height 8.4 m/s (which is from the measurements of the upstream tower). A detailed description of the EOLOS turbine and analysis of this period data can be found in [23].

In the computation, a fully developed turbulent boundary layer flow is fed at the inlet. The lengths of the computational domain are 1500 meters, 800 meters and 1000 meters in the streamwise (x), spanwise (y) and vertical (z) directions, respectively. The mesh near the turbine and in turbine near-wake is uniform with a grid spacing of 5 meters. The numbers of grid nodes are 201, 121 and 121 in x, y and z directions, respectively. 51 points are employed along the line for each blade. The time step is $0.044s$. Three cases are carried out: fixed ω, fixed TSR, and generator torque control. For the fixed TSR case, the inflow velocity for calculating ω is taken at hub height 1.67D upstream of the turbine. The distance 1.67D is chosen as this is the upstream distance of the met tower from the turbine at the EOLOS field station. The computations were first carried out until the total kinetic energy of the computational domain reached a quasi-steady state, and subsequently the flow fields were averaged for approximately 20 minutes.

Simulations with uniform inflow were carried out first at different fixed TSR and with different values of K_g in the generator torque control. In Figure 2, we compare the computed C_P of these simulations with those predicted from Blade-element theory, which should work well for uniform inflow. Good agreements are obtained for both simulations with fixed TSR and generator torque control.

The inlet profiles for the turbulent inflow cases are shown in Figure 3. Good agreements with the measurements are obtained for the mean streamwise velocity. However, the turbulence

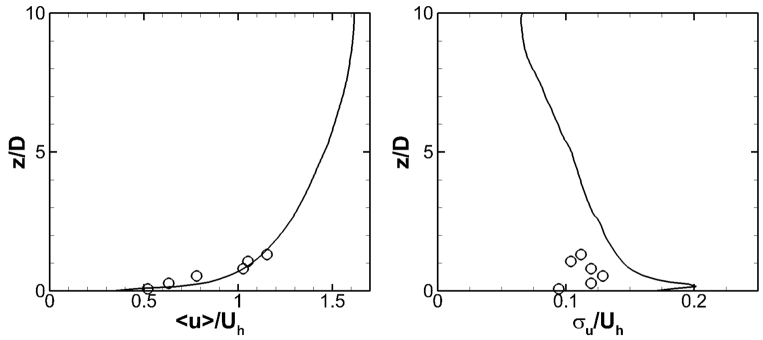

Figure 3: Vertical profiles of the streamwise velocity (a) and turbulence intensity σ_u at the inlet for turbulent inflow cases.

	ω (rad/s)	TSR	P (MW)	P_{rms}	τ_{aero} $(Nm \times 10^6)$	τ_{aero}^{rms} $(Nm \times 10^6)$
Fixed ω	1.43	8.43	1.21	0.45	0.81	0.31
Fixed TSR	1.50	8.65	1.20	0.43	0.76	0.19
Torque control	1.46	8.49	1.22	0.41	0.79	0.20
Measurements	1.51	8.37	1.21	0.19	0.79*	0.09*

*The aerodynamic torque is calculated by P/ω, where P and ω are the measured values.

Table 1: Summary of the computed results from the three cases: fixed ω, fixed TSR and generator torque control.

intensity σ_u is over predicted. The computed results from the three cases with turbulent inflow are summarized in Table 1, in which the power is calculated by:

$$P = \tau_{aero}\omega \tag{6}$$

As seen, the time-averaged power and aerodynamic torque from the computation agree well with the measurements for all the three cases. However the rms (root-mean-square) of the power and aerodynamic torque fluctuations from the computation are larger than that from measurements. This is probably because the turbulence intensity of the inflow is higher for the simulation (Figure 3 (b)). It is also observed that the rms of the aerodynamic torque fluctuations from the case with fixed ω is significantly higher than that from the other two cases. The reason for this observation, however, is still not clear.

The time-averaged flow fields from the generator torque control are shown in Figure 4. The flow fields from the three cases are nearly the same (not shown). Some minor differences are observed for the turbulence kinetic energy in the far wake as shown in Figure 5 (c).

4. Summary

Generator torque control has been implemented in an actuator line model. The computed power coefficients agree well with the ones calculated from the blade-element theory for uniform inflow. The model has also been applied to EOLOS wind turbine with turbulent inflow. Three cases have been carried out: fixed turbine rotating speed, fixed TSR and generator torque control. The time-averaged flow fields from the three cases are nearly the same. Good agreement is obtained for the time-averaged power for all three cases. Significantly larger root-mean-square

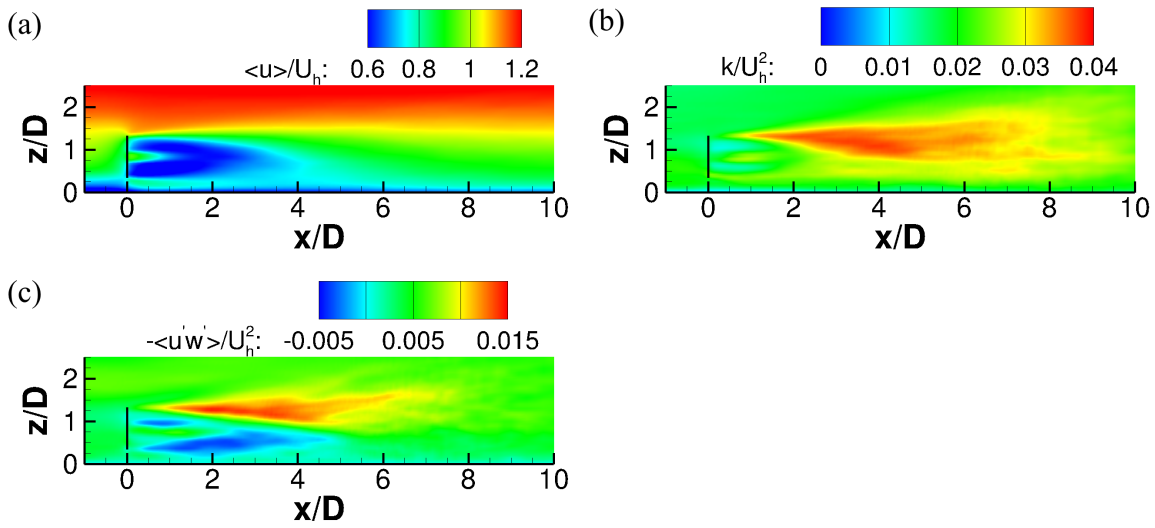

Figure 4: Time-averaged flow fields from the case with generator torque control for (a) streamwise velocity, (b) turbulence kinetic energy and (c) primary Reynolds shear stress.

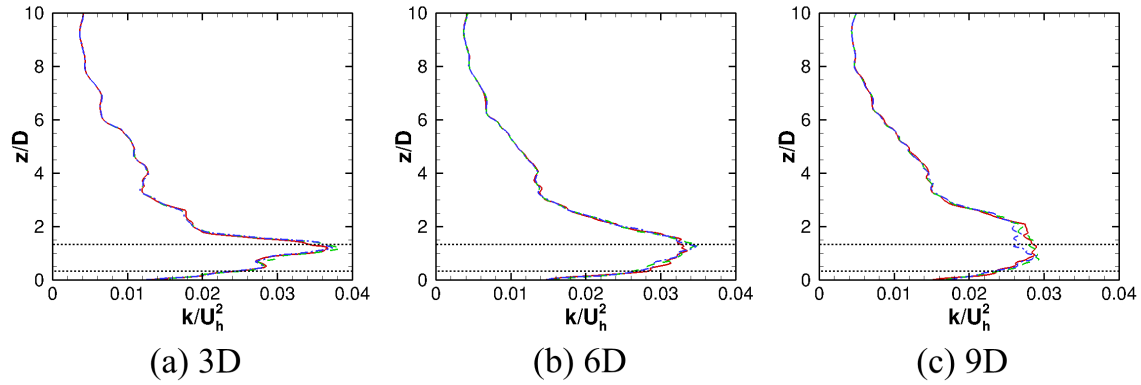

Figure 5: Vertical profiles of turbulence kinetic energy at 3D (a), 6D (b) and 9D (c) downstream from the turbine. Red solid line: fixed ω; green dashed line: fixed TSR; blue dash-dot line: generator torque control.

(rms) of the aerodynamic torque fluctuations is observed for the case with fixed ω. The reason for this will be investigated in the future work.

In addition to a generator torque controller, turbines typically have a blade pitch controller at or above rated wind speeds. This controller holds generator torque constant and pitches the blades to minimize structural loads. A blade pitch controller was not considered in this paper, but will be incorporated in future work.

Acknowledgments

This work was supported by Department of Energy DOE (DE-EE0002980, DE-EE0005482 and DE-AC04-94AL85000) and University of Minnesota Initiative for Renewable Energy and the Environment IREE (grant no RO-0004-12). This work was also supported by the National Science Foundation under Grant No. NSF-CMMI-1254129 entitled CAREER: Probabilistic Tools for High Reliability Monitoring and Control of Wind Farms. Any opinions, findings, and conclusions or recommendations expressed in this material are those of the authors and

do not necessarily reflect the views of the NSF. Computational resources were provided by the University of Minnesota Supercomputing Institute.

References

[1] Storey R, Norris S, Stol K and Cater J 2013 *Wind Energy* **16** 845–864
[2] Jonkman J M and Buhl Jr M L 2005 *Golden, CO: National Renewable Energy Laboratory*
[3] Churchfield M, Moriarty P, Vijayakumar G and Brasseur J 2010 *National Renewable Energy Laboratory, Golden, CO, Report No. NREL/CP-500-48905*
[4] Churchfield M J, Lee S, Michalakes J and Moriarty P J 2012 *Journal of Turbulence*
[5] Lee S, Churchfield M, Moriarty P, Jonkman J and Michalakes J 2013 *Journal of Solar Energy Engineering* **135** 031001
[6] Churchfield M J, Lee S, Moriarty P J, Martinez L A, Leonardi S, Vijayakumar G and Brasseur J G 2012 *AIAA paper*
[7] OpenCFD Reading B U Opencfd, openfoam the open source cfd toolbox, users manual, version 1.7.1 Tech. rep.
[8] Archer C L, Mirzaeisefat S and Lee S 2013 *Geophysical Research Letters* **40** 4963–4970
[9] Maché M, Mouslim H and Mervoyer L 2014 From meso-scale to micro scale les modelling: Application by a wake effect study for an offshore wind farm *ITM Web of Conferences* vol 2 (EDP Sciences) p 01004
[10] Keck R E, Maré M, Churchfield M J, Lee S, Larsen G and Madsen H A 2013 *Wind Energy*
[11] Keck R E, Maré M, Churchfield M J, Lee S, Larsen G and Aagaard Madsen H 2013 *Wind Energy*
[12] Fleming P, Gebraad P, Lee S, van Wingerden J, Johnson K, Churchfield M, Michalakes J, Spalart P and Moriarty P 2013 *Proceedings of ICOWES 2013*
[13] Ge L and Sotiropoulos F 2007 *J. Comput. Phys.* **225** 1782–1809
[14] Germano M, Piomelli U, Moin P and Cabot W H 1991 *Phys. Fluids A* **3** 1760–1765
[15] Kang S, Lightbody A, Hill C and Sotiropoulos F 2011 *Adv. Water Resour.* **34** 98–113
[16] Sørensen J N and Shen W Z 2002 *J. Fluid Eng. Trans. ASME* **124** 393–399
[17] Yang X, Zhang X, Li Z and He G W 2009 *Journal of Computational Physics* **228** 7821–7836
[18] Yang X, Kang S and Sotiropoulos F 2012 *Physics of Fluids* **24** 115107 (pages 28)
[19] Yang X and Sotiropoulos F 2013 On the predictive capabilities of les-actuator disk model in simulating turbulence past wind turbines and farms *American Control Conference (ACC), 2013* (IEEE) pp 2878–2883
[20] Johnson K E, Pao L Y, Balas M J and Fingersh L J 2006 *Control Systems, IEEE* **26** 70–81
[21] Pao L Y and Johnson K E 2011 *Control Systems, IEEE* **31** 44–62
[22] Burton T, Jenkins N, Sharpe D and Bossanyi E 2011 *Wind energy handbook* (John Wiley & Sons)
[23] Chamorro L P, Lee S J, Olsen D, Milliren C, Marr J, A Arndt R and Sotiropoulos F *Wind Energy*